Supplementary Material

Identification of Blood Biomarkers Related to Energy Metabolism and Construction of Diagnostic Prediction Model Based on Three Independent Alzheimer's Disease Cohorts

Supplementary Table 1. Characteristics of the patients included in the cohort set.

	Control	AD	*p*
GSE63060			
No.	104	145	
Sex, n (%)			0.1797
Male	42 (40.38%)	46 (31.72%)	
Female	62 (59.62%)	99 (68.28%)	
Age			
y (SD)	72.38 ± 6.339	75.40 ± 6.581	0.0003
GSE63061			
No.	134	139	
Sex, n (%)			>0.9999
Male	53 (39.55%)	54 (38.85%)	
Female	81 (60.45%)	85 (61.15%)	
Age			
y (SD)	75.29 ± 6.024	77.89 ± 6.667	0.0008
Single center			
No.	12	13	
Sex, n (%)			0.0154
Male	8 (66.67%)	2 (15.38%)	
Female	4 (33.33%)	11 (84.62%)	
Age			
y (SD)	62.00 ± 10.830	86.38 ± 5.910	<0.0001

AD, Alzheimer's disease; No, n, number; SD, standard deviation. The age difference is presented as mean ± SD and compared using t-test. The gender difference is presented with the frequency and percentage, and compared using the Chi-Square and Fisher's exact test.

Supplementary Table 2. Summary of key genes/proteins and family homologues in AD and other diseases.

Gene or protein	Disease or model	Mechanism	Reference
RPL26	AD	Oxidative phosphorylation	Wang et al.[1]
RPL26, NDUFA1	AD	Immune infiltration	Zhuang et al.[2]
MECOM	AML	Evi1 regulates genes related to cellular-energy-related pathways, including glycolysis, the TCA cycle and oxidative phosphorylation, purine and pyrimidine synthesis, and the metabolism of various amino acids.	Fenouille et al.[3]
mRPL10	AED	Glycolysis and mitochondrial function have been found to be affected by ribosomal availability.	Li et al.[4]
RPL22	Melanoma	Ribosome recruitment regulated HIF1A mRNAs, cell viability, glucose uptake and lactate release.	Rapino et al.[5]
RPL26, RPS27	Laryngeal squamous carcinoma	Proliferation inhibition and enhanced survivability of cells	Liu et al.[6]
RPL26, RPS10	PHT cell	The expression of trophoblast genes involved in ribosome and protein synthesis, mitochondrial function, lipid metabolism is regulated by mTORC1	Rosario et al.[7]

TCA, tricarboxylic acid; AML, acute myeloid leukemia; RPL22, ribosomal protein L22; mRPL10, Mitochondrial Ribosomal Protein L10; AED, abnormal eye development PHT, primary human trophoblast.

Supplementary Table 3. The sequences of the primers.

Gene symbol	Primer	Sequences (5’-3’)
NDUFA1	Forward primer	CATCCACAGGTTCACTAA
	Reverse primer	CTATCTCTTTCCATCAGACT
MECOM	Forward primer	ATACAGCAATCATTCCATT
	Reverse primer	TCAGCAATAGAAGCAATAG
RPS27	Forward primer	AGAAGAGGAGAAGAGGAA
	Reverse primer	TAAAGACCGTGGTGATTT
RPL26	Forward primer	TGGTTATCACTAGGCTAA
	Reverse primer	ATCTTCTCAATGGTTTCTT
PINK1	Forward primer	CCTCGTTATGAAGAACTATCCCTG
	Reverse primer	GGATGTTGTCGGATTTCAGGTC
GAPDH	Forward primer	AGGTCGGAGTCAACGGATTT
	Reverse primer	TGACGGTGCCATGGAATTTG

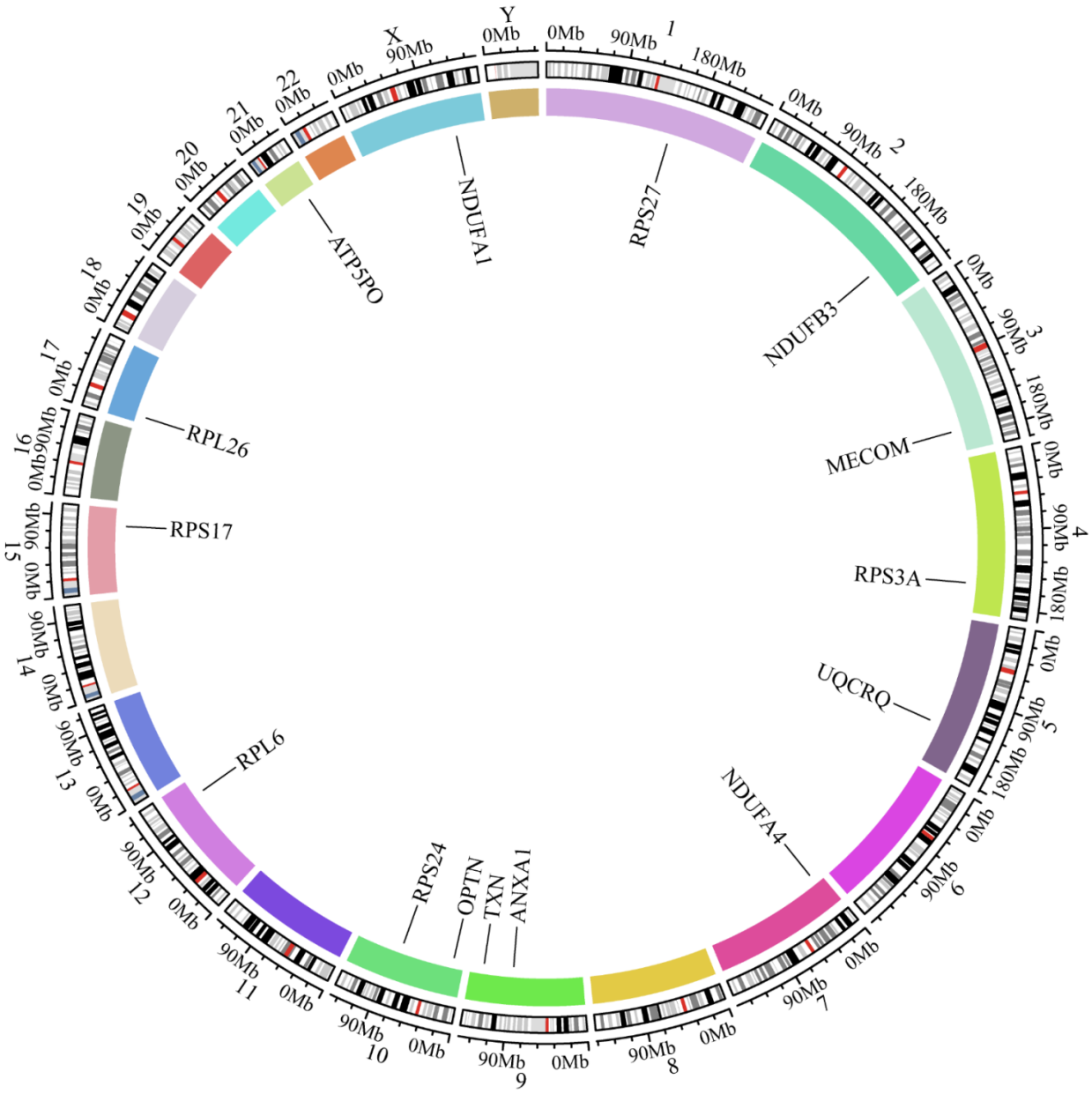

Supplementary Figure 1. Circos plot for mapping the location of 15 key genes on the chromosomes.

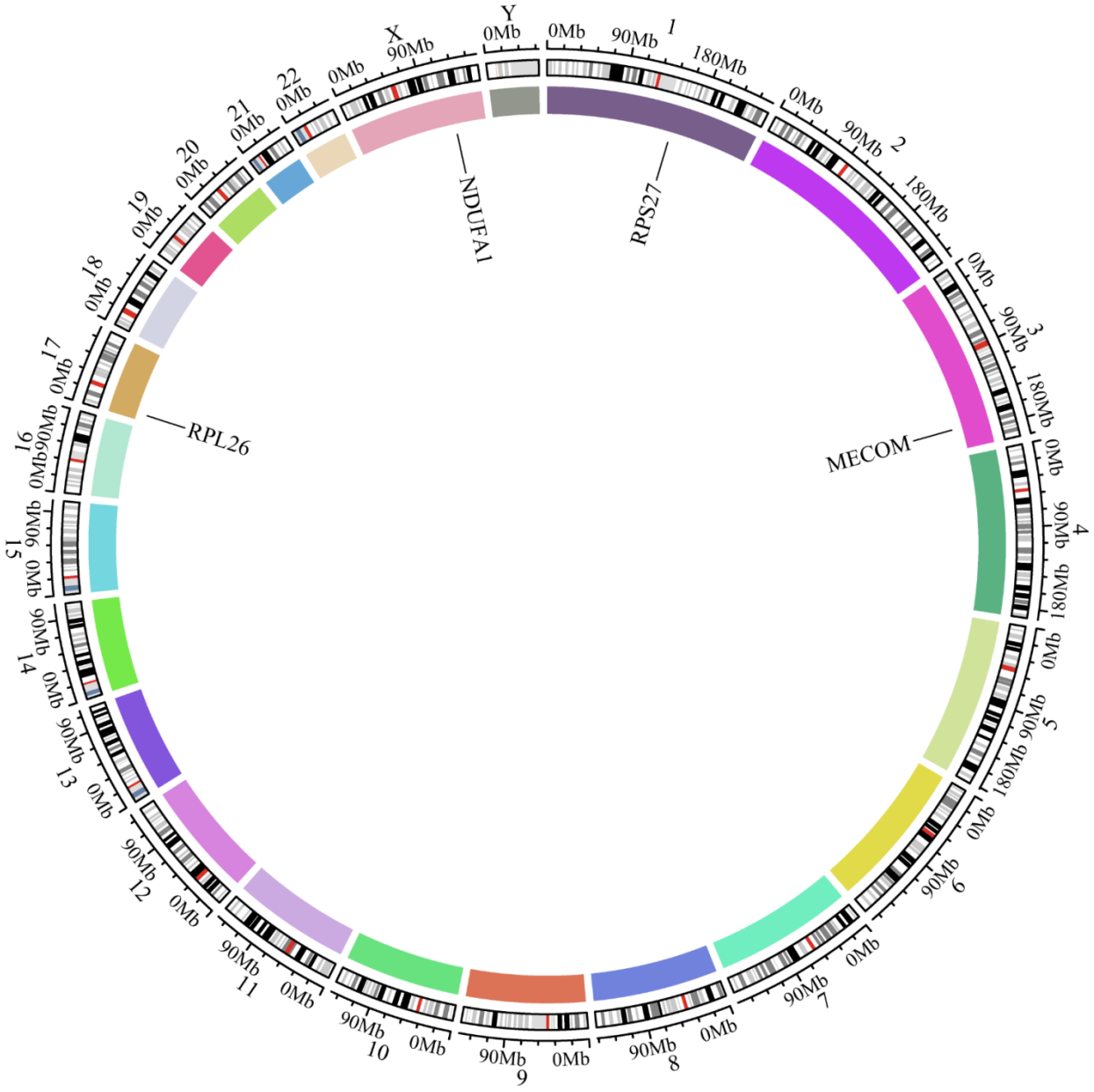

Supplementary Figure 2. Circos plot for mapping the location of 4 biomarkers on the chromosomes.

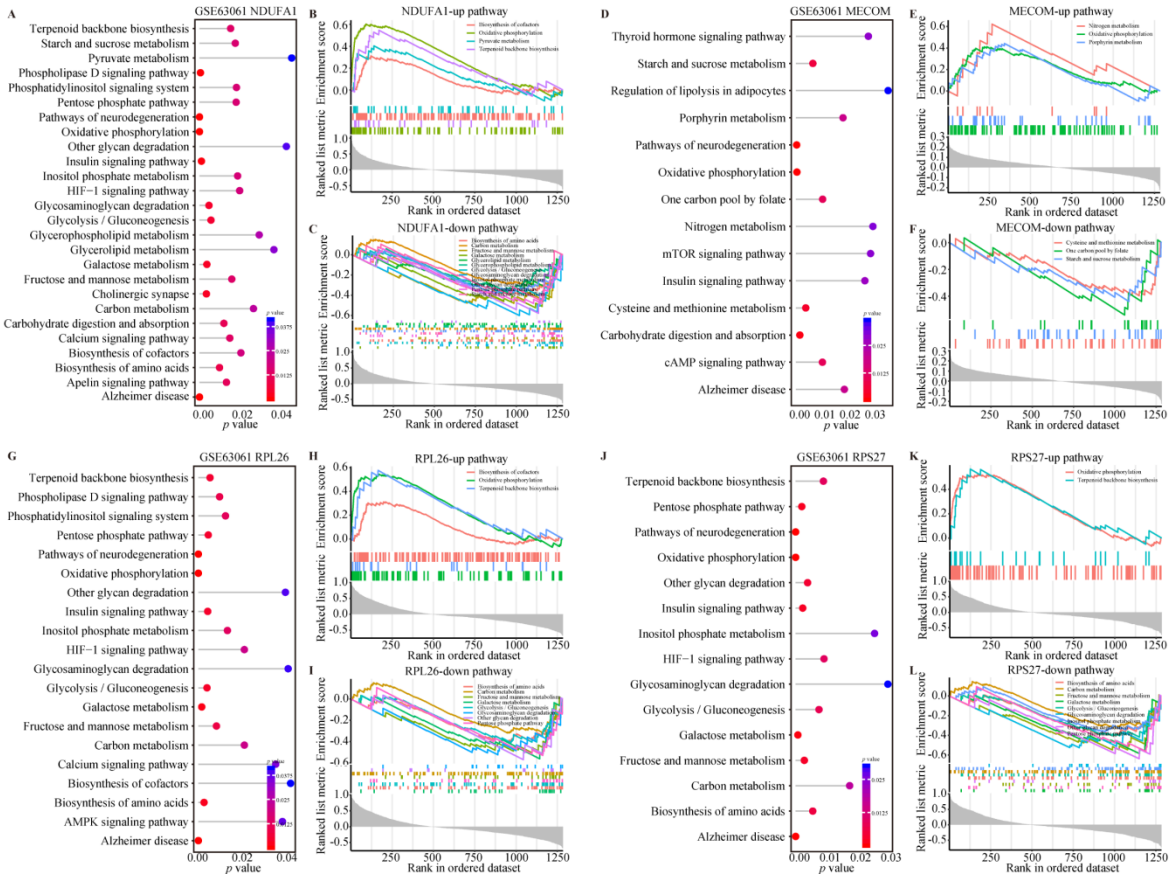

Supplementary Figure 3. Metabolism and energy metabolism pathways of 4 biomarkers in GSE63061 cohort. A-L) Single gene GSVA analysis based on KEGG pathway enrichment of *NDUFA1*, *MECOM*, *RPL26*, and *RPS27*. Lollipop plots of 4 biomarkers KEGG pathway enrichment results in the left of each panel. The horizontal and the color indicate the *p* value. GSEA plots in the right of each panel shows the metabolism and energy metabolism related pathways with different colors for 4 biomarkers. All presented pathways were significantly enrichened. Statistical significance is $p < 0.05$.

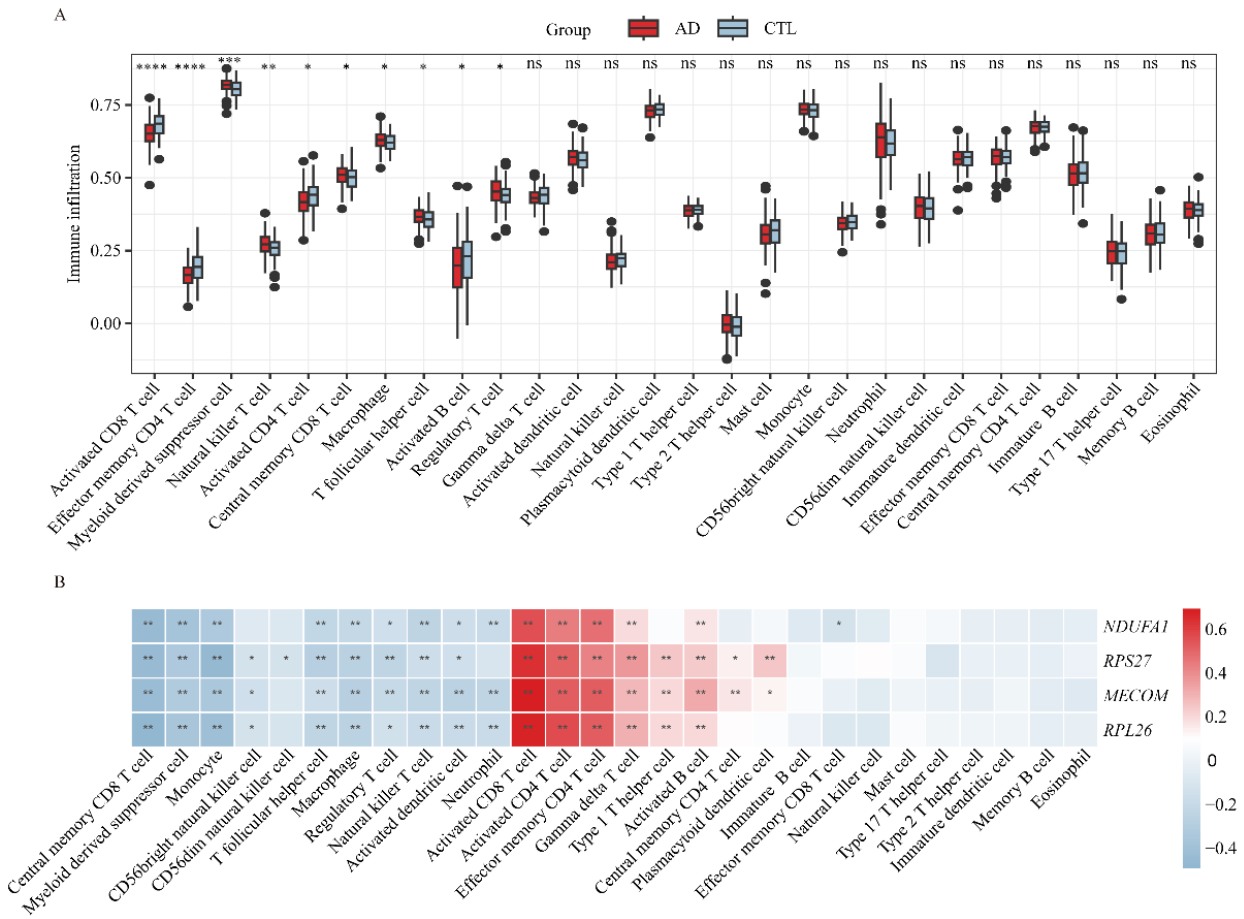

Supplementary Figure 4. Immune characteristics and correlation analysis of AD and biomarkers. A) Immune cell characteristics boxplots between AD and CTL (*p < 0.05, **p < 0.01, ***p < 0.001, ****p < 0.0001 vs. the control group). CTL, control; AD, Alzheimer's disease; ns, no significance. B) Heatmap of correlation between biomarkers and immune cells. Red represents positive correlation; blue represents negative correlation (*p < 0.05, **p < 0.01). Statistical comparisons were carried out with Wilcoxon rank-sum test. The correlation was analyzed by Spearman's correlation method.

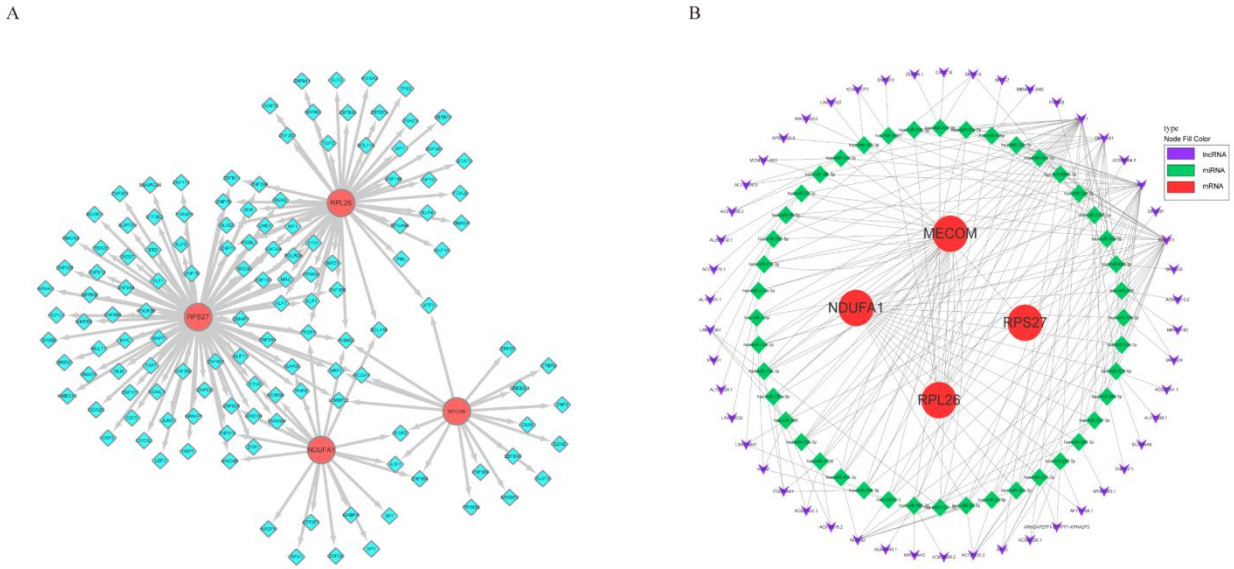

Supplementary Figure 5. Global landscape of TF and ceRNA regulatory network centered on AD biomarkers. A) TF-biomarker network construction to reveal the regulatory interaction on the protein levels. Blue squares represent TFs, and red nodes present AD biomarkers. B) The ceRNA interaction regulatory network across AD biomarkers. Red nodes indicate AD biomarkers. Green squares indicate miRNAs, and purple arrows indicate lncRNAs.

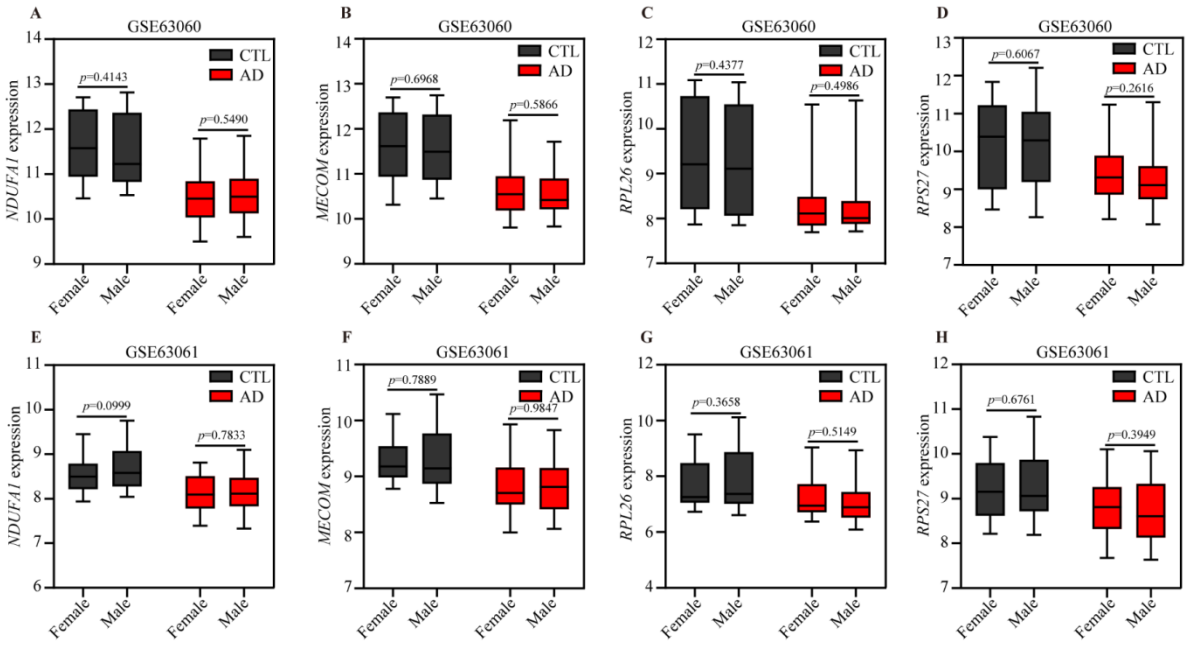

Supplementary Figure 6. The expression levels of AD biomarkers in both genders. A-H) The expression levels of 4 blood biomarkers (*NDUFA1*, *MECOM*, *RPL26*, and *RPS27*) in different genders of the GSE63060 cohort (A-D) and GSE63061 cohort (E-H). CTL, control; AD, Alzheimer's disease. Box plots represent the median, 25th and 75th percentiles and whiskers represent the 5th and 95th percentiles. Statistical comparisons were carried out with t test (GSE63060 cohort, CTL, female *n* = 62, male, *n* = 42; AD, female *n* = 99, male, *n* = 46. GSE63061 cohort, CTL, female *n* = 81, male, *n* = 53; AD, female *n* = 85, male, *n* = 53).

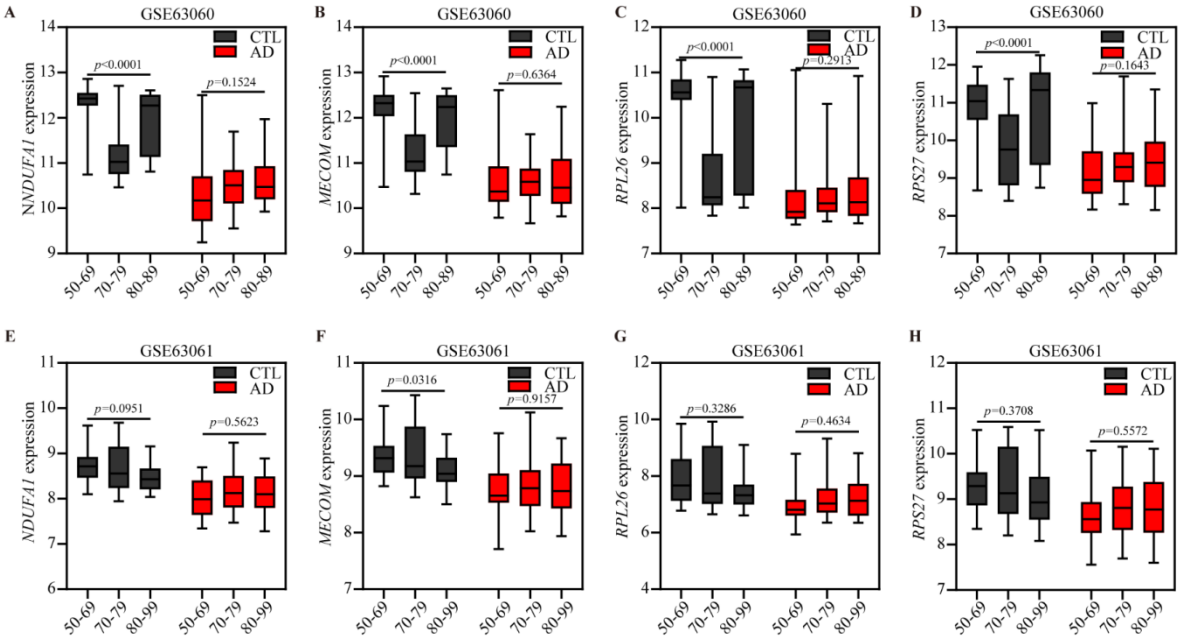

Supplementary Figure 7. The expression levels of AD biomarkers in different age ranges. A-H) The expression levels of AD biomarkers in different age ranges of participants in the GSE63060 cohort (A-D) and GSE63061 cohort (E-H). CTL, control; AD, Alzheimer's disease. Box plots represent the median, 25th and 75th percentiles and whiskers represent the 5th and 95th percentiles. Statistical comparisons of the 4 blood biomarkers modules by age grouping were assessed by one-way ANOVA (GSE63060 cohort, for CTL, Total *n* = 104; 50-69 y, *n* = 32; 70-79 y, *n* = 63; 80-99 y, *n* = 9; for AD, Total *n* = 145; 59-69 y, *n* = 24; 70-79 y, *n* = 77; 80-99 y, *n* = 44. GSE63061 cohort, for CTL, Total *n* = 134; 59-69 y, *n* = 23; 70-79 y, *n* = 77; 80-99 y, *n* = 34; for AD: Total *n* = 139; 59-69 y, *n* = 16; 70-79 y, *n* = 62; 80-99 y, *n* = 61).

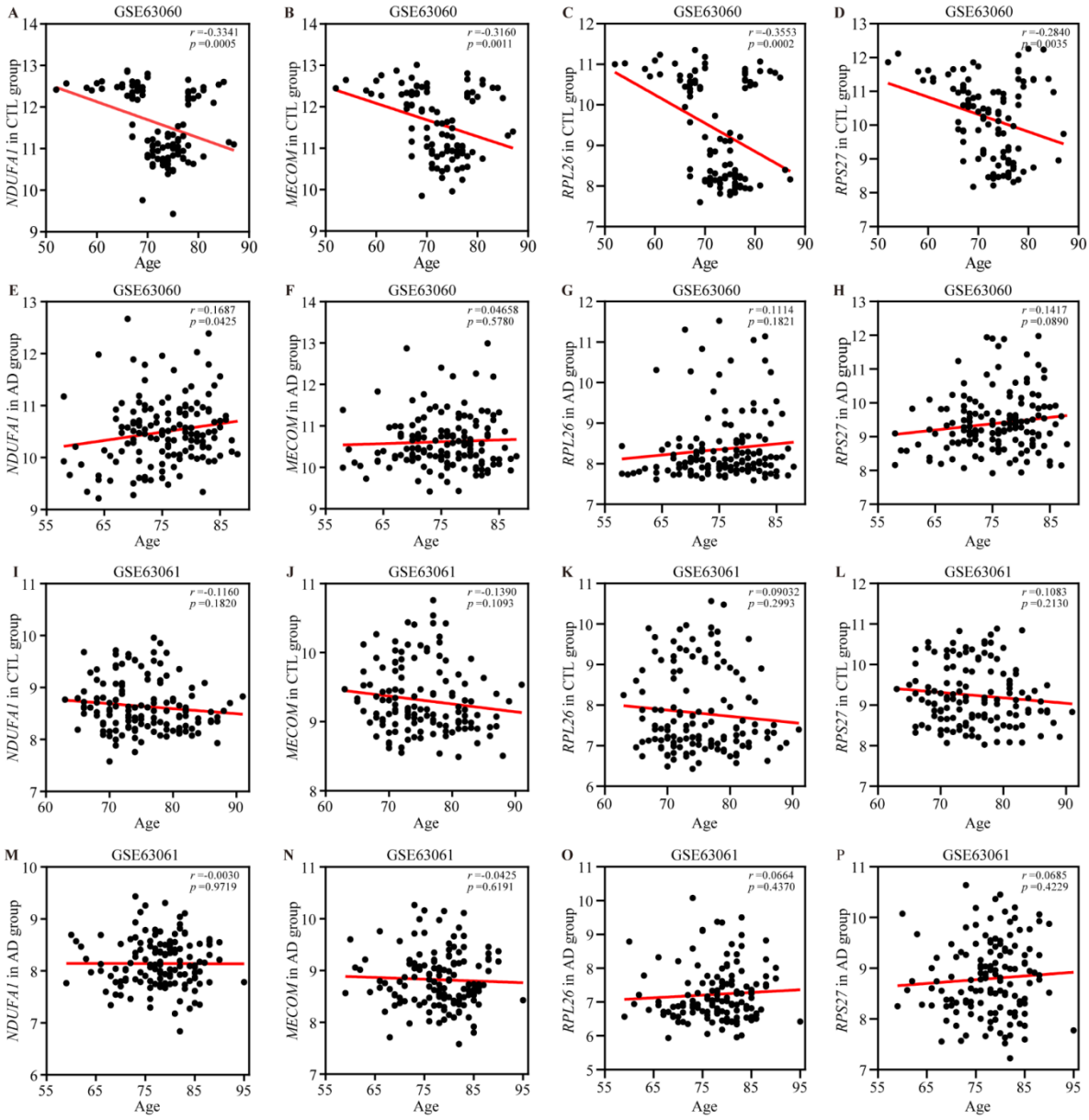

Supplementary Figure 8. Effects of aging on potential AD blood biomarkers. A-P) Correlation analysis of blood biomarkers (NDUFA1, MECOM, RPL26, and RPS27) and aging in the GSE63060 cohort (A-H) and GSE63061 cohort (I-P). CTL, control; AD, Alzheimer's disease. The scatters represent AD participants and the red lines represent the fitting line for correlation. The correlation analysis between the 4 biomarkers and age was performed using Pearson's correlation test (GSE63060 cohort, CTL, *n* = 104, 52-87 y; AD, *n* = 145, 58-88 y; GSE63061 cohort, CTL, *n* = 134, 63-91 y; AD, *n* = 139, 59-95 y).

m

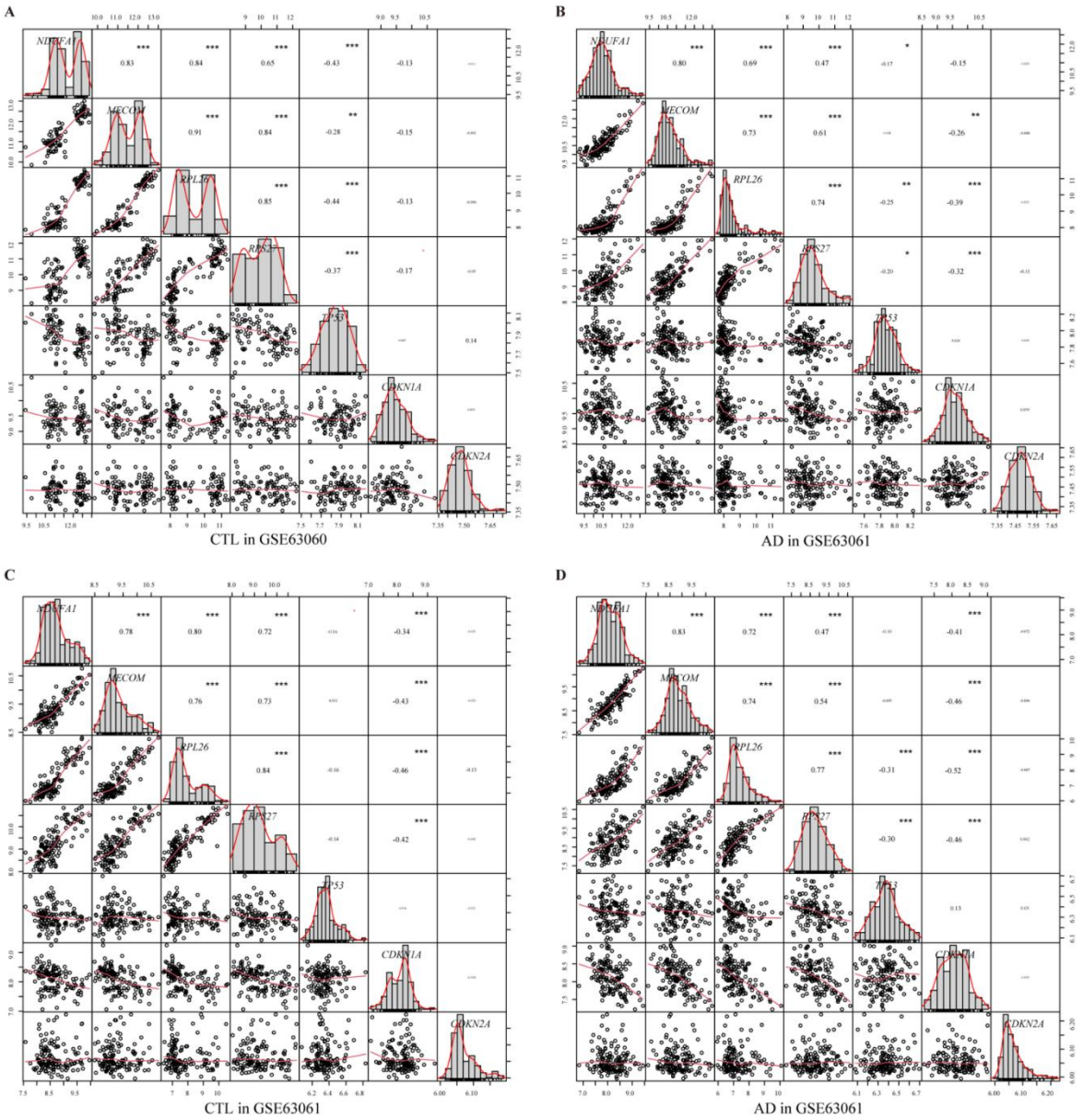

Supplementary Figure 9. Correlation plots for biomarkers and aging factors. A-D) The correlation analysis of 4 biomarkers (NDUFA1, MECOM, RPL26, and RPS27) and 3 aging factors (TP53, CDKN1A, and CDKN2A) in control and AD cohorts of the GSE63060 cohort (A-B) and GSE63061 cohort (C-D). CTL, control; AD, Alzheimer's disease. Correlations were carried out with Spearman's correlation test (*$p < 0.05$, **$p < 0.01$, ***$p < 0.001$).

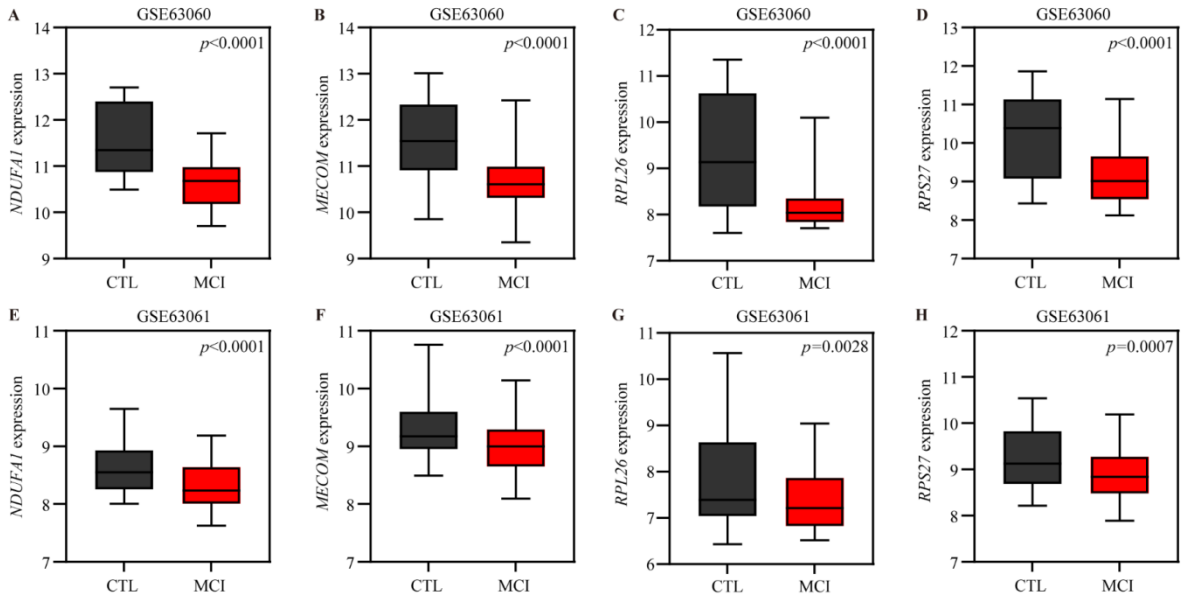

Supplementary Figure 10. The expression levels of AD biomarkers in control and MCI groups. A-D) The expression levels of AD biomarkers in the control and MCI participants from the GSE63060 cohort. E-H) The expression levels of AD biomarkers in the control and MCI participants from the GSE63061 cohort. CTL, control; MCI, mild cognition impairment. The black for control and the red for MCI. Box plots represent the median, 25th and 75th percentiles and whiskers represent the 5th and 95th percentiles. Statistical comparisons were carried out with t test (GSE63060 cohort, CTL, *n* = 104, MCI, *n* = 80; GSE63061 cohort, CTL, *n* = 134, MCI, *n* = 115).

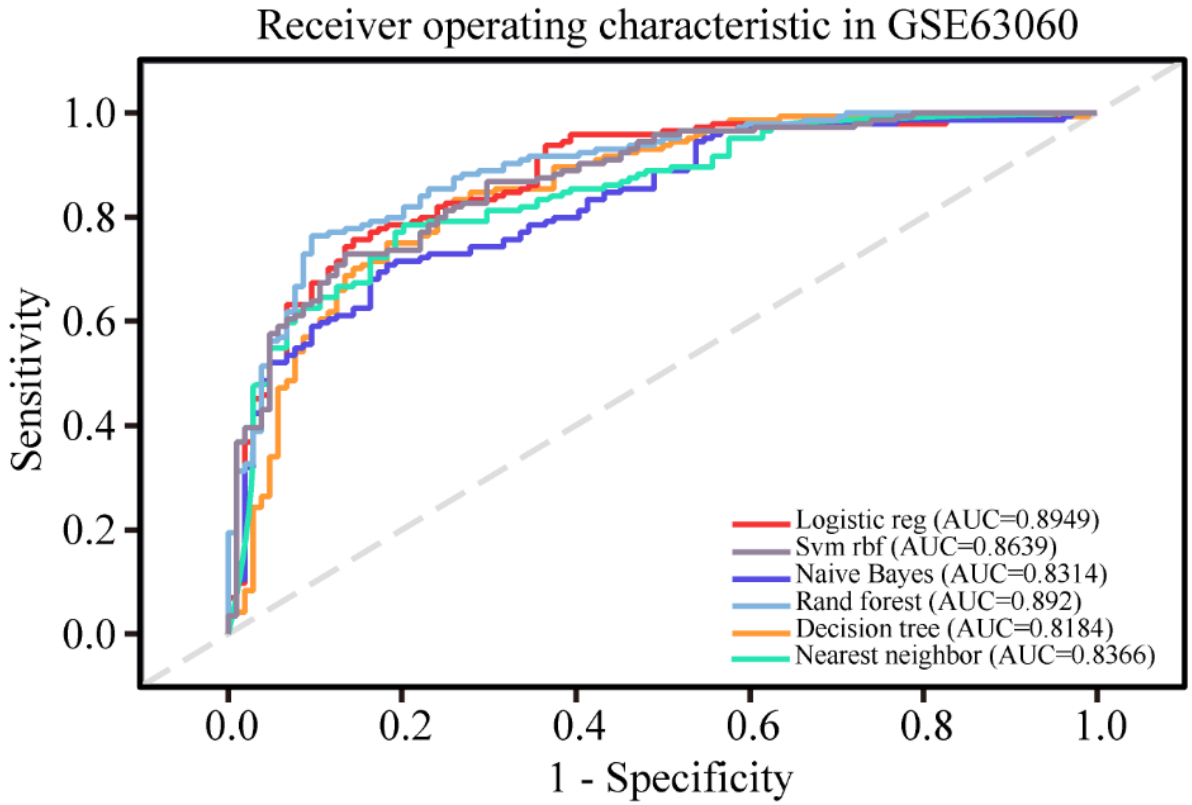

Supplementary Figure 11. Multiple machine learning algorithms validation on AD biomarkers nomogram. Machine learning algorithms for training cohort GSE63060.

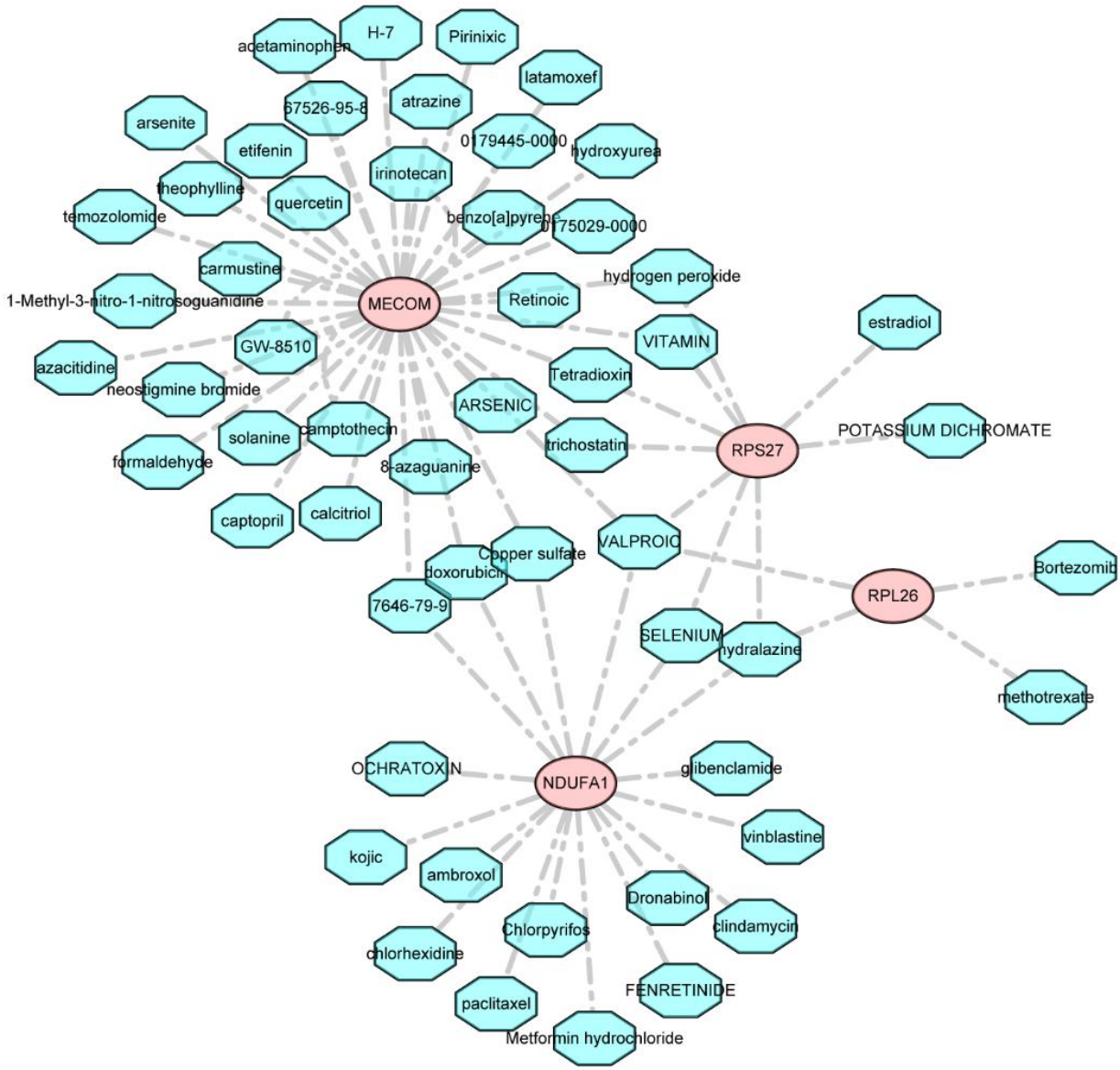

Supplementary Figure 12. Potential drug prediction of AD biomarkers from DSigDB. Blue hexagons for drugs, and pink ellipses for AD biomarkers.

REFERENCES

1. Wang H, Han X and Gao S. Identification of potential biomarkers for pathogenesis of Alzheimer's disease. *Hereditas* 2021; 158: 23. 20210705.
2. Zhuang X, Zhang G, Bao M, et al. Development of a novel immune infiltration-related diagnostic model for Alzheimer's disease using bioinformatic strategies. *Front Immunol* 2023; 14: 1147501.
3. Fenouille N, Bassil CF, Ben-Sahra I, et al. The creatine kinase pathway is a metabolic vulnerability in EVI1-positive acute myeloid leukemia. *Nat Med* 2017; 23: 301-313.
4. Li HB, Wang RX, Jiang HB, et al. Mitochondrial ribosomal protein L10 associates with cyclin B1/Cdk1 activity and mitochondrial function. *DNA Cell Biol* 2016; 35: 680-690.
5. Rapino F, Delaunay S, Rambow F, et al. Codon-specific translation reprogramming promotes resistance to targeted therapy. *Nature* 2018; 558: 605-609.
6. Liu J, Ma T, Gao M, et al. Proteomic characterization of proliferation inhibition of well-differentiated laryngeal squamous cell carcinoma cells under below-background radiation in a deep underground environment. *Front Public Health* 2020; 8: 584964.
7. Rosario FJ, Powell TL, Gupta MB, et al. mTORC1 transcriptional regulation of ribosome subunits, protein synthesis, and molecular transport in primary human trophoblast cells. *Front Cell Dev Biol* 2020; 8: 583801.